Search for a massive invisible particle X^{0} in B^{+}→e^{+}X^{0} and B^{+}→μ^{+}X^{0} decays

C.-S. Park *et al.* (Belle Collaboration)

Phys. Rev. D **94**, 012003 — Published 18 July 2016

DOI: 10.1103/PhysRevD.94.012003

Search for a massive invisible particle X^0 in $B^+ \to e^+ X^0$ and $B^+ \to \mu^+ X^0$ decays

C.-S. Park,[69] Y.-J. Kwon,[69] I. Adachi,[12,9] H. Aihara,[61] D. M. Asner,[47] T. Aushev,[35] V. Babu,[55] I. Badhrees,[54,24] A. M. Bakich,[53] E. Barberio,[33] P. Behera,[16] V. Bhardwaj,[51] J. Biswal,[21] G. Bonvicini,[67] A. Bozek,[42] M. Bračko,[31,21] T. E. Browder,[11] D. Červenkov,[5] V. Chekelian,[32] A. Chen,[39] B. G. Cheon,[10] K. Chilikin,[34] R. Chistov,[34] K. Cho,[25] V. Chobanova,[32] Y. Choi,[52] D. Cinabro,[67] J. Dalseno,[32,56] M. Danilov,[34] N. Dash,[14] Z. Doležal,[5] D. Dutta,[55] S. Eidelman,[4,45] H. Farhat,[67] J. E. Fast,[47] T. Ferber,[7] B. G. Fulsom,[47] V. Gaur,[55] N. Gabyshev,[4,45] A. Garmash,[4,45] R. Gillard,[67] Y. M. Goh,[10] P. Goldenzweig,[23] O. Grzymkowska,[42] T. Hara,[12,9] K. Hayasaka,[37] H. Hayashii,[38] M. Heck,[23] W.-S. Hou,[41] T. Iijima,[37,36] K. Inami,[36] G. Inguglia,[7] A. Ishikawa,[59] R. Itoh,[12,9] Y. Iwasaki,[12] I. Jaegle,[11] H. B. Jeon,[27] T. Julius,[33] K. H. Kang,[27] E. Kato,[59] P. Katrenko,[35] D. Y. Kim,[50] J. B. Kim,[26] K. T. Kim,[26] M. J. Kim,[27] S. H. Kim,[10] K. Kinoshita,[6] P. Kodyš,[5] S. Korpar,[31,21] P. Križan,[70,21] P. Krokovny,[4,45] A. Kuzmin,[4,45] I. S. Lee,[10] C. H. Li,[33] L. Li,[48] Y. Li,[66] L. Li Gioi,[32] J. Libby,[16] D. Liventsev,[66,12] M. Lubej,[21] P. Lukin,[4,45] M. Masuda,[60] D. Matvienko,[4,45] K. Miyabayashi,[38] H. Miyata,[43] R. Mizuk,[34,35] G. B. Mohanty,[55] S. Mohanty,[55,65] A. Moll,[32,56] H. K. Moon,[26] R. Mussa,[20] E. Nakano,[46] M. Nakao,[12,9] K. J. Nath,[15] M. Nayak,[16] K. Negishi,[59] N. K. Nisar,[55,1] S. Nishida,[12,9] S. Ogawa,[58] S. Okuno,[22] P. Pakhlov,[34] G. Pakhlova,[35] B. Pal,[6] C. W. Park,[52] H. Park,[27] T. K. Pedlar,[30] M. Petrič,[21] L. E. Piilonen,[66] C. Pulvermacher,[23] M. V. Purohit,[51] J. Rauch,[57] M. Ritter,[29] A. Rostomyan,[7] S. Ryu,[49] Y. Sakai,[12,9] S. Sandilya,[55] L. Santelj,[12] T. Sanuki,[59] Y. Sato,[36] T. Schlüter,[29] O. Schneider,[28] G. Schnell,[2,13] C. Schwanda,[18] A. J. Schwartz,[6] Y. Seino,[43] D. Semmler,[8] K. Senyo,[68] O. Seon,[36] M. E. Sevior,[33] V. Shebalin,[4,45] C. P. Shen,[3] T.-A. Shibata,[62] J.-G. Shiu,[41] B. Shwartz,[4,45] F. Simon,[32,56] A. Sokolov,[19] S. Stanič,[44] M. Starič,[21] J. Stypula,[42] T. Sumiyoshi,[63] U. Tamponi,[20,64] Y. Teramoto,[46] K. Trabelsi,[12,9] M. Uchida,[62] T. Uglov,[35] Y. Unno,[10] S. Uno,[12,9] P. Urquijo,[33] Y. Usov,[4,45] C. Van Hulse,[2] P. Vanhoefer,[32] G. Varner,[11] K. E. Varvell,[53] M. N. Wagner,[8] C. H. Wang,[40] M.-Z. Wang,[41] P. Wang,[17] Y. Watanabe,[22] E. Won,[26] J. Yamaoka,[47] S. Yashchenko,[7] H. Ye,[7] Y. Yook,[69] Y. Yusa,[43] Z. P. Zhang,[48] V. Zhilich,[4,45] V. Zhulanov,[4,45] and A. Zupanc[70,21]

(The Belle Collaboration)

[1] *Aligarh Muslim University, Aligarh 202002*
[2] *University of the Basque Country UPV/EHU, 48080 Bilbao*
[3] *Beihang University, Beijing 100191*
[4] *Budker Institute of Nuclear Physics SB RAS, Novosibirsk 630090*
[5] *Faculty of Mathematics and Physics, Charles University, 121 16 Prague*
[6] *University of Cincinnati, Cincinnati, Ohio 45221*
[7] *Deutsches Elektronen–Synchrotron, 22607 Hamburg*
[8] *Justus-Liebig-Universität Gießen, 35392 Gießen*
[9] *SOKENDAI (The Graduate University for Advanced Studies), Hayama 240-0193*
[10] *Hanyang University, Seoul 133-791*
[11] *University of Hawaii, Honolulu, Hawaii 96822*
[12] *High Energy Accelerator Research Organization (KEK), Tsukuba 305-0801*
[13] *IKERBASQUE, Basque Foundation for Science, 48013 Bilbao*
[14] *Indian Institute of Technology Bhubaneswar, Satya Nagar 751007*
[15] *Indian Institute of Technology Guwahati, Assam 781039*
[16] *Indian Institute of Technology Madras, Chennai 600036*
[17] *Institute of High Energy Physics, Chinese Academy of Sciences, Beijing 100049*
[18] *Institute of High Energy Physics, Vienna 1050*
[19] *Institute for High Energy Physics, Protvino 142281*
[20] *INFN - Sezione di Torino, 10125 Torino*
[21] *J. Stefan Institute, 1000 Ljubljana*
[22] *Kanagawa University, Yokohama 221-8686*
[23] *Institut für Experimentelle Kernphysik, Karlsruher Institut für Technologie, 76131 Karlsruhe*
[24] *King Abdulaziz City for Science and Technology, Riyadh 11442*
[25] *Korea Institute of Science and Technology Information, Daejeon 305-806*
[26] *Korea University, Seoul 136-713*
[27] *Kyungpook National University, Daegu 702-701*
[28] *École Polytechnique Fédérale de Lausanne (EPFL), Lausanne 1015*

[29]Ludwig Maximilians University, 80539 Munich
[30]Luther College, Decorah, Iowa 52101
[31]University of Maribor, 2000 Maribor
[32]Max-Planck-Institut für Physik, 80805 München
[33]School of Physics, University of Melbourne, Victoria 3010
[34]Moscow Physical Engineering Institute, Moscow 115409
[35]Moscow Institute of Physics and Technology, Moscow Region 141700
[36]Graduate School of Science, Nagoya University, Nagoya 464-8602
[37]Kobayashi-Maskawa Institute, Nagoya University, Nagoya 464-8602
[38]Nara Women's University, Nara 630-8506
[39]National Central University, Chung-li 32054
[40]National United University, Miao Li 36003
[41]Department of Physics, National Taiwan University, Taipei 10617
[42]H. Niewodniczanski Institute of Nuclear Physics, Krakow 31-342
[43]Niigata University, Niigata 950-2181
[44]University of Nova Gorica, 5000 Nova Gorica
[45]Novosibirsk State University, Novosibirsk 630090
[46]Osaka City University, Osaka 558-8585
[47]Pacific Northwest National Laboratory, Richland, Washington 99352
[48]University of Science and Technology of China, Hefei 230026
[49]Seoul National University, Seoul 151-742
[50]Soongsil University, Seoul 156-743
[51]University of South Carolina, Columbia, South Carolina 29208
[52]Sungkyunkwan University, Suwon 440-746
[53]School of Physics, University of Sydney, NSW 2006
[54]Department of Physics, Faculty of Science, University of Tabuk, Tabuk 71451
[55]Tata Institute of Fundamental Research, Mumbai 400005
[56]Excellence Cluster Universe, Technische Universität München, 85748 Garching
[57]Department of Physics, Technische Universität München, 85748 Garching
[58]Toho University, Funabashi 274-8510
[59]Department of Physics, Tohoku University, Sendai 980-8578
[60]Earthquake Research Institute, University of Tokyo, Tokyo 113-0032
[61]Department of Physics, University of Tokyo, Tokyo 113-0033
[62]Tokyo Institute of Technology, Tokyo 152-8550
[63]Tokyo Metropolitan University, Tokyo 192-0397
[64]University of Torino, 10124 Torino
[65]Utkal University, Bhubaneswar 751004
[66]CNP, Virginia Polytechnic Institute and State University, Blacksburg, Virginia 24061
[67]Wayne State University, Detroit, Michigan 48202
[68]Yamagata University, Yamagata 990-8560
[69]Yonsei University, Seoul 120-749
[70]Faculty of Mathematics and Physics, University of Ljubljana, 1000 Ljubljana

We present a search for a non-Standard-Model invisible particle X^0 in the mass range 0.1-1.8 GeV/c^2 in $B^+ \to e^+ X^0$ and $B^+ \to \mu^+ X^0$ decays. The results are obtained from a 711 fb^{-1} data sample that corresponds to $772 \times 10^6 B\bar{B}$ pairs, collected at the $\Upsilon(4S)$ resonance with the Belle detector at the KEKB e^+e^- collider. One B meson is fully reconstructed in a hadronic mode to determine the momentum of the lepton of the signal decay in the rest frame of the recoiling partner B meson. We find no evidence of a signal and set upper limits on the order of 10^{-6}.

PACS numbers: 13.20.-v, 14.60.st, 14.80.Nb

Since the theoretical proposal by Pauli [1] and the discovery by Cowan *et al.* [2], neutrinos have played a crucial role in developing and shaping the standard model (SM) of elementary particle physics. Recent observation of neutrino oscillation [3] requires that they have non-zero masses. But in the minimal SM, there is no mechanism for them to acquire non-zero mass.

Many new physics models beyond the SM introduce heavy neutrinos to explain neutrino masses through the so-called seesaw mechanism [4]. Moreover, these heavy neutrinos can help explain dark matter in the universe. It is of great interest to search for heavy neutrino-like particles. Such a heavy neutrino is an invisible particle, which we denote X^0, and can be studied in B^+ decays to l^+X^0 [5], where l denotes an electron or muon.

There are further possibilities for the X^0 candidate in hypotheses of new physics beyond the SM. One is sterile neutrinos in large extra dimensions [6] and in the neutrino minimal standard model (νMSM) that incorporate the three light singlet right-handed fermions [7]. Another option is the lightest supersymmetric particle (LSP) in the minimal supersymmetric standard model (MSSM) [8] assuming R-parity violation. If the X^0 is the LSP, it can be a neutralino that is produced via the process shown in Fig. 1. If we observe a particle X^0 that is significantly heavier than an SM neutrino, it would indicate new physics.

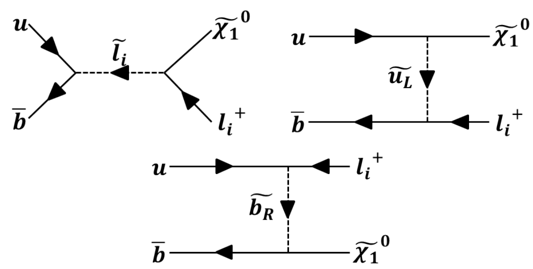

FIG. 1: Some Feynman diagrams to produce the lightest neutralino from B meson decays in MSSM assuming R-parity violation.

In this article, we report on searches for $B^+ \to e^+ X^0$ and $B^+ \to \mu^+ X^0$ decays with an X^0 mass in the range 0.1 to $1.8\,\mathrm{GeV}/c^2$. The searches use an $e^+e^- \to \Upsilon(4S)$ data sample of $711\,\mathrm{fb}^{-1}$ containing 772×10^6 $B\bar{B}$ events produced by the KEKB [9] asymmetric e^+e^- collider at $\sqrt{s} = 10.58\,\mathrm{GeV}$, which is at the $\Upsilon(4S)$ resonance, and recorded with the Belle detector.

The Belle detector is a large-solid-angle magnetic spectrometer that consists of a silicon vertex detector, a 50-layer central drift chamber (CDC), an array of aerogel threshold Čerenkov counters (ACC), a barrel-like arrangement of time-of-flight scintillation counters, and an electromagnetic calorimeter comprised of CsI(Tl) crystals (ECL) located inside a super-conducting solenoid coil that provides a 1.5 T magnetic field. An iron flux-return yoke located outside of the coil is instrumented to detect K_L^0 mesons and to identify muons (KLM). The detector is described in detail elsewhere [10].

We assume the X^0 is invisible and has a lifetime long enough to escape from the Belle detector. Assuming a mean X^0 lifetime of 10^{-6} seconds, fewer than 1% of X^0 decay in the detector. We search for a signal by exploiting the two-body decay kinematics of $B^+ \to l^+ X^0$ decays. The magnitude p_l^B of the momentum of the charged lepton measured in the rest frame of the parent B^+ meson depends on the X^0 mass. The resolution of p_l^B is affected by the unknown direction of the parent B^+. To improve this resolution, we fully reconstruct the other B meson in the event in a hadronic decay mode. For this reconstruction, an algorithm based on hierarchical neural networks [11] is used. The charged B meson, thus reconstructed with 615 exclusive decay channels, is labeled B_{tag} and is used to constrain the kinematics of the signal B meson. The B_{tag} reconstruction quality for each candidate is denoted by a variable o_{tag}, which is the output from the neural network algorithm. This variable takes the value from zero to unity, and is interpreted as a measure of the probability that B_{tag} candidate is correctly reconstructed.

When there are multiple B_{tag} candidates in an event, we choose the candidate that has the largest o_{tag} value from the hadronic tagging algorithm. We require $o_{\mathrm{tag}} > 0.0025$, for which the purity of the tagged B^+ sample is 73%; this falls to 56% if we select a B_{tag} candidate randomly regardless of o_{tag}. To suppress combinatorially formed B_{tag} candidates, we further require the following conditions on the energy difference $\Delta E = E_{B_{\mathrm{tag}}} - \sqrt{s}/2$, and the beam-energy-constrained mass $M_{\mathrm{bc}} = \sqrt{(s/4)/c^4 - |\vec{p}_{B_{\mathrm{tag}}}|^2/c^2}$, where $\vec{p}_{B_{\mathrm{tag}}}$ and $E_{B_{\mathrm{tag}}}$ are the reconstructed momentum and energy, respectively, of the B_{tag} candidate in the center-of-mass (CM) frame: $M_{\mathrm{bc}} > 5.27$ GeV$/c^2$ and $|\Delta E| < 0.05$ GeV.

The efficiency, ϵ_{tag}, of hadronic B tagging is initially determined by Monte Carlo (MC) simulation, then corrected for a small data-MC difference by analyzing control sample modes composed of the semileptonic $B^+ \to \bar{D}^{(*)0} l^+ \nu_l$ decays. For $\bar{D}^0 l^+ \nu_l$, we consider only the $\bar{D}^0$ decays to $K^+\pi^-$, $K^+\pi^-\pi^0$, and $K^+\pi^-\pi^+\pi^-$. For $\bar{D}^{*0} l^+ \nu_l$, we use $\bar{D}^{*0}$ decays to $\bar{D}^0\pi^0$ and $\bar{D}^0\gamma$ with $\bar{D}^0 \to K^+\pi^-$.

We calculate the weighted average of the correction factors determined from each control mode with their branching fractions as weights, as described in Ref. [12]. After the correction, the efficiency of the B_{tag} reconstruction is 0.17% for $B^+ \to e^+ X^0$ and 0.18% for $B^+ \to \mu^+ X^0$, with the relative uncertainty of ϵ_{tag} being 6.4% [13].

After removing particles used in the B_{tag} reconstruction, we require that an event have only one charged track, that its charge be opposite that of the B_{tag} and that its laboratory-frame momentum exceed 1.0 GeV$/c$. This charged track is required to satisfy $|dz| < 2.0\,\mathrm{cm}$ and $dr < 0.5\,\mathrm{cm}$, where $|dz|$ and dr are the distances of closest approach to the interaction point along and perpendicular to the beam axis.

We require that this charged track be identified as an electron or a muon. Electrons are identified by means of a likelihood ratio based on the following information: the ratio between the cluster energy in the ECL and the track momentum from the CDC (E/p), the specific ionization dE/dx in the CDC, the position and shower shape of the cluster in the ECL and the response from the ACC. Muon identification uses the matching information between the charged track and the KLM-hit positions as well as the KLM penetration depth. With our track selection criteria, the electron and muon efficiencies are over 90% and their hadron misidentification rates are below 0.5% and 5%, respectively. A more detailed description of the lepton identification can be found in Ref. [14].

The continuum background events ($e^+e^- \to q\bar{q}$ with $q = u, d, s, \mathrm{or}\, c$) are suppressed using the event shape difference between $B\bar{B}$ and continuum events. In the CM frame, due to the low momentum of the B mesons, the event shape of a $B\bar{B}$ event tends to be more spherical while the continuum backgrounds tend to be more jet-like. To exploit this difference, we use the cosine of the thrust angle, $\cos\theta_{\rm T}$, to suppress the continuum backgrounds. Here, $\theta_{\rm T}$ is the angle between the thrust axis of the $B_{\rm tag}$ and the momentum of the signal-side lepton in the CM frame; the thrust axis is the direction that maximizes the sum of the longitudinal momenta of the particles [15]. We apply $|\cos\theta_{\rm T}| < 0.9$ and $|\cos\theta_{\rm T}| < 0.8$ for electron and muon candidates, relatively. The more stringent condition is used for the muon due to its larger misidentification probability.

The remaining backgrounds, especially those with extra neutral particles from the signal B meson side, are suppressed by using the variable $E_{\rm ECL}$, which is defined as the sum of the extra energy in the ECL beyond that associated with the $B_{\rm tag}$ constituents and the signal-side lepton. In calculating $E_{\rm ECL}$, we consider only clusters with energies above 50 MeV in the barrel, 100 MeV in the forward endcap, and 150 MeV in the backward endcap [10]. The higher thresholds in the endcap regions reflect the more severe beam background in those regions. We require $E_{\rm ECL} < 0.5\,{\rm GeV}$ to enhance the signal.

We determine the signal yield and the amount of background contamination by using the variable p_l^B. Figure 2 shows the MC expectation for signal and background for p_l^B between $1.8\,{\rm GeV}/c$ and $2.8\,{\rm GeV}/c$. The p_l^B distributions of the signal MC events are displayed for the three cases: $M_{X^0} = 0.1,\ 1.0$ and $1.8\ {\rm GeV}/c^2$. The background level becomes increasingly significant as p_l^B falls below $2.3\,{\rm GeV}/c$.

As a result, we restrict our search to $M_{X^0} \leq 1.8\,{\rm GeV}/c^2$, beyond which the search sensitivity is greatly degraded due to background. For each assumed value of M_{X^0}, the p_l^B signal region is optimized based on the expected upper limit of the signal branching fraction, which is estimated by MC simulation. Considering the width of the so optimized signal regions of p_l^B in Table I, we perform the search in $0.1\,{\rm GeV}/c^2$ steps of M_{X^0}, whereby the entire test region ($0.1\,{\rm GeV}/c^2 \leq M_{X^0} \leq 1.8\,{\rm GeV}/c^2$) is covered without any gaps.

The number of expected background events in the p_l^B signal region is estimated by first performing a maximum likelihood fit to p_l^B in the region $1.8\,{\rm GeV}/c < p_l^B < 2.25\,{\rm GeV}/c$ ("sideband"), where we expect very little contribution from the signal events for $M_{X^0} < 1.8\,{\rm GeV}/c^2$. The fitted yield is then extrapolated to the p_l^B signal region, which is discussed in more detail below. To fit the p_l^B sideband, we consider the following sources of background: continuum, $b \to c$ decays, semileptonic $b \to ul\nu$ decays, and other rare and leptonic B-decay processes. The background distributions are modelled by the probability density functions (PDFs), which are described in Table II. We do not consider continuum background in the fitting because it is almost completely removed by our pre-selection. Note that we utilize separate PDFs for the $B^+ \to l^+\nu_l\gamma$, $B^+ \to \pi^0 l^+\nu_l$, and $B^+ \to \pi^+ K^0$ decays, as these modes show peaking behavior in the p_l^B distribution. The $B^+ \to l^+\nu_l\gamma$ modes

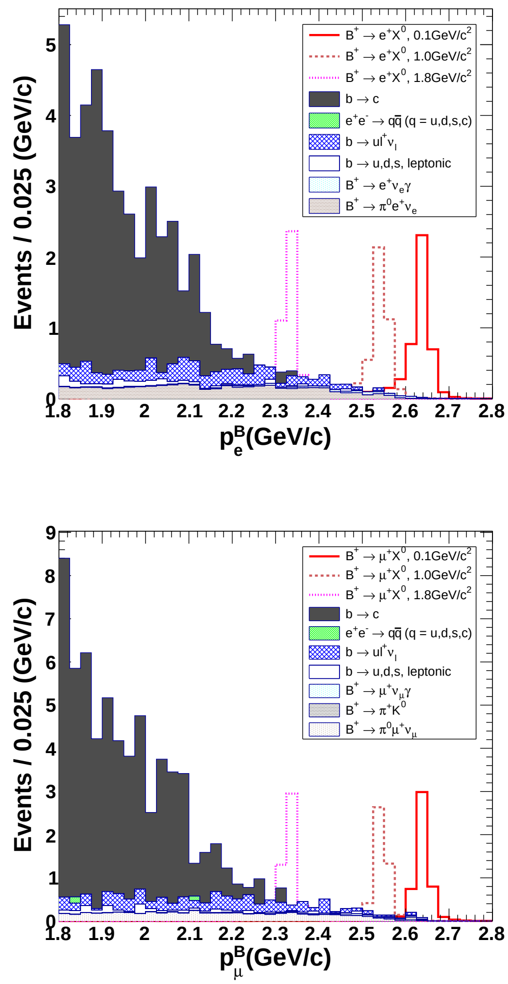

FIG. 2: p_l^B MC distributions for $B^+ \to e^+X^0$ (top) and $B^+ \to \mu^+X^0$ (bottom), where signal MC is arbitrary scaled. The $e^+e^- \to q\bar{q}$ background is negligible. $B^+ \to e^+\nu_e\gamma$, $B^+ \to \mu^+\nu_\mu\gamma$ and $B^+ \to \pi^+K^0$ backgrounds become important for $p_l^B > 2.5\,{\rm GeV}/c$.

(excluding taus), which have not been observed, could produce a substantial yield of high-momentum leptons near the signal regions, so we simulate them with dedicated large-sample-size MC. We use a branching fraction of 2×10^{-6} for $B^+ \to e^+\nu_e\gamma$ and $B^+ \to \mu^+\nu_\mu\gamma$, which is lower than the recently measured upper limit [16]. For $B^+ \to \pi^0 l^+\nu_l$, $B^+ \to \pi^+K^0$ and $B^+ \to l^+\nu_l\gamma$, high-statistics MC samples are produced with 300, 500, and 2500 times, respectively, more integrated luminosity than the data. In the fit, only the overall normalization is free and the relative yields of all background modes are fixed based on the measured or assumed branching fractions. Finally, the number of background events extrapolated in each signal region is corrected by the data-MC difference. The correction factor is calculated as the ratio of the number of events in the corresponding p_l^B signal region in the $E_{\rm ECL}$ sideband ($1.8\,{\rm GeV}/c < p_l^B < 3.0\,{\rm GeV}/c$, $0.5\,{\rm GeV} < E_{\rm ECL} < 2.0\,{\rm GeV}$) in data and in the MC sample. The range of correction factors is 1.10 - 1.11 for the electron mode and 0.93 - 0.99 for the muon mode.

The signal branching fractions are obtained by the following equation:

$$\mathcal{B}(B^+ \to l^+ X^0) = \frac{N_{\rm obs} - N_{\rm exp}^{\rm bkg}}{2 \cdot \epsilon_{\rm s} \cdot N_{B^+B^-}}, \quad (1)$$

where $N_{\rm obs}$ is the number of observed events and $N_{\rm exp}^{\rm bkg}$ is the number of expected background events, both in the p_l^B signal region, $\epsilon_{\rm s}$ is the signal efficiency, and $N_{B^+B^-} = (396 \pm 7) \times 10^6$ is the number of B^+B^- events. The factor of 2 in the denominator appears because we search for signals in both B^+ and B^- decays (see [5]).

To evaluate $\epsilon_{\rm s}$, signal MC samples are generated using EvtGen [18], including final-state radiation using PHOTOS [19]. These samples are processed with a detector simulation based on GEANT3 [20]. The signal efficiencies are summarized in Table I.

Figure 3 shows the p_l^B distribution of the on-resonance data. The fitted yield of background in the p_l^B sideband of on-resonance data is extrapolated to the signal region. The extrapolation factor is determined from background MC samples.

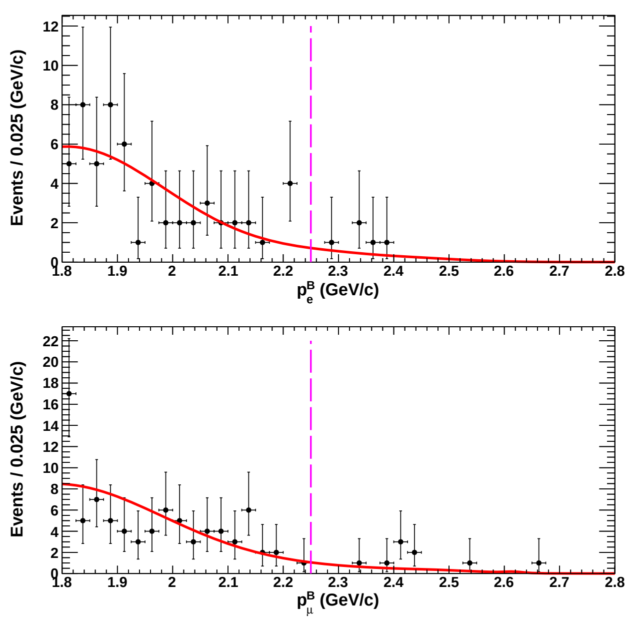

FIG. 3: p_l^B data distributions for $B^+ \to e^+X^0$ (top) and $B^+ \to \mu^+X^0$ (bottom), where the red curve indicates the background expectation and the magenta dashed line indicates the upper bound of the p_l^B sideband.

The observed yields in the signal region are summarized in Table I. There is no signal excess for either mode in any M_{X^0} range. In the muon mode for $M_{X^0} = 1.5\,{\rm GeV}/c^2$ ($1.6\,{\rm GeV}/c^2$), we find 5 (4) events in the p_l^B signal region while we expect 1.12 ± 0.34 (0.95 ± 0.29) background events. The local p-value of this yield, assuming a background-only hypothesis, is 0.60%(1.59%). We obtain the 90% confidence level (CL) upper limit of the signal yield in each case by using the frequentist approach [21] implemented in the POLE (Poissonian limit estimator) program [22], where the systematic uncertainties are taken into account.

The systematic uncertainty consists of the multiplicative uncertainty on $\epsilon_{\rm s} \cdot N_{B^+B^-}$ and the additive uncertainty on the background. The multiplicative uncertainty is calculated from the uncertainties on the number of B^+B^- events, track finding and lepton identification for the signal lepton, the $\epsilon_{\rm tag}$ correction, the p_l^B shape, and the signal MC sample size.

A 1.8% uncertainty is assigned for the uncertainty on the number of B mesons and the branching fraction of $\Upsilon(4S) \to B^+B^-$ [23]. The track-finding uncertainty is estimated by comparing the track-finding efficiency in data and MC, determining it in both cases from the number of pions in the partially and fully reconstructed $D^* \to \pi D^0$, $D^0 \to \pi\pi K_S^0$, $K_S^0 \to \pi\pi$ decay chain. For the p_l^B shape uncertainty, we use the 3.6% uncertainty from the $B^+ \to \bar{D}^0\pi^+$ control sample study in the $B^+ \to l^+\nu_l$ search [13] due to its similar kinematics. The lepton identification uncertainty is estimated by comparing the efficiency difference between data and MC using $\gamma\gamma \to l^+l^-$. The multiplicative systematic uncertainties are summarized in Table III.

The systematic uncertainties on the background estimation are determined by considering the following sources: uncertainties in the background PDF parameters, the branching fraction of the background modes and the statistical uncertainty from the p_l^B sideband. Each source is varied one at a time by its uncertainty ($\pm 1\sigma$) and the resulting deviations from the nominal background yield are added in quadrature. For the branching fraction uncertainties of the background modes, we use the world-average values in Ref. [23] for $B^+ \to \pi^0 l^+\nu_l$ and $B^+ \to \pi^+ K^0$. For $B^+ \to l^+\nu_l\gamma$, a variation of $\pm 50\%$ is applied. For other modes, where an estimate of the background level is not clearly available, a conservative branching fraction uncertainty of $^{+100}_{-50}\%$ is assumed.

More than 95% of $b \to c$ decays result in observed $D^{(*)}l^+\nu_l$ final states, so we use their branching fraction uncertainties [23]. The values of $N_{\rm exp}^{\rm bkg}$ and their uncertainties for both $B^+ \to e^+X^0$ and $B^+ \to \mu^+X^0$ are listed in Table I.

Figure 4 shows the expected and obtained 90% CL upper limits of $\mathcal{B}(B^+ \to l^+X^0)$ for each assumed value of M_{X^0}. Table I summarizes the p_l^B signal region, estimated background, signal efficiency, number of observed events, and upper limit of the branching fraction at 90% CL for each assumed value of M_{X^0} for both modes.

From the branching fraction upper limits, assuming R-parity violation, we can set bounds on the MSSM-related

TABLE I: Summary of the signal efficiency (ϵ_s), the number of events observed in the p_l^B signal region ($N_{\rm obs}$), the number of expected background yield in the signal region ($N_{\rm exp}^{\rm bkg}$), and the upper limit of the branching fraction at 90% CL ($\mathcal{B}^{90}$) for the $B^+ \to l^+ X^0$ searches. Also shown is the p_l^B signal region for each assumption of M_{X^0} and the mode.

M_{X^0} (GeV/c^2)	p_l^B signal region (GeV/c)	$\epsilon_{\rm s}$ (%)	$N_{\rm obs}$	$N_{\rm exp}^{\rm bkg}$	$\mathcal{B}^{90}$
			$B^+ \to e^+ X^0$ mode		
0.1	2.52–2.70	0.11	0	0.36 ± 0.13	$< 2.4 \times 10^{-6}$
0.2	2.52–2.70	0.11	0	0.36 ± 0.13	$< 2.4 \times 10^{-6}$
0.3	2.55–2.68	0.11	0	0.21 ± 0.13	$< 2.6 \times 10^{-6}$
0.4	2.55–2.68	0.11	0	0.21 ± 0.08	$< 2.7 \times 10^{-6}$
0.5	2.52–2.70	0.11	0	0.36 ± 0.08	$< 2.5 \times 10^{-6}$
0.6	2.52–2.70	0.11	0	0.36 ± 0.13	$< 2.5 \times 10^{-6}$
0.7	2.52–2.70	0.11	0	0.36 ± 0.13	$< 2.4 \times 10^{-6}$
0.8	2.51–2.62	0.11	0	0.37 ± 0.12	$< 2.5 \times 10^{-6}$
0.9	2.51–2.62	0.10	0	0.37 ± 0.12	$< 2.6 \times 10^{-6}$
1.0	2.51–2.62	0.096	0	0.37 ± 0.12	$< 2.8 \times 10^{-6}$
1.1	2.47–2.57	0.099	0	0.58 ± 0.18	$< 2.4 \times 10^{-6}$
1.2	2.45–2.53	0.096	0	0.61 ± 0.19	$< 2.5 \times 10^{-6}$
1.3	2.43–2.51	0.098	0	0.72 ± 0.22	$< 2.3 \times 10^{-6}$
1.4	2.41–2.51	0.10	0	0.97 ± 0.30	$< 2.0 \times 10^{-6}$
1.5	2.39–2.46	0.093	1	0.85 ± 0.27	$< 4.8 \times 10^{-6}$
1.6	2.37–2.43	0.092	1	0.84 ± 0.27	$< 4.9 \times 10^{-6}$
1.7	2.34–2.39	0.088	1	0.85 ± 0.28	$< 5.1 \times 10^{-6}$
1.8	2.31–2.36	0.087	2	1.01 ± 0.34	$< 7.1 \times 10^{-6}$
			$B^+ \to \mu^+ X^0$ mode		
0.1	2.58–2.68	0.12	1	0.37 ± 0.14	$< 4.3 \times 10^{-6}$
0.2	2.58–2.68	0.12	1	0.37 ± 0.14	$< 4.2 \times 10^{-6}$
0.3	2.58–2.68	0.12	1	0.37 ± 0.14	$< 4.3 \times 10^{-6}$
0.4	2.58–2.68	0.12	1	0.37 ± 0.14	$< 4.3 \times 10^{-6}$
0.5	2.58–2.68	0.11	1	0.37 ± 0.14	$< 4.4 \times 10^{-6}$
0.6	2.58–2.68	0.11	1	0.37 ± 0.14	$< 4.6 \times 10^{-6}$
0.7	2.56–2.63	0.11	0	0.39 ± 0.13	$< 2.4 \times 10^{-6}$
0.8	2.54–2.61	0.11	1	0.41 ± 0.15	$< 4.4 \times 10^{-6}$
0.9	2.52–2.60	0.11	1	0.52 ± 0.18	$< 4.3 \times 10^{-6}$
1.0	2.49–2.58	0.11	1	0.74 ± 0.25	$< 4.1 \times 10^{-6}$
1.1	2.49–2.58	0.12	1	0.74 ± 0.25	$< 3.9 \times 10^{-6}$
1.2	2.48–2.53	0.10	0	0.54 ± 0.17	$< 2.4 \times 10^{-6}$
1.3	2.45–2.50	0.10	0	0.67 ± 0.21	$< 2.3 \times 10^{-6}$
1.4	2.42–2.48	0.11	2	0.90 ± 0.28	$< 5.8 \times 10^{-6}$
1.5	2.40–2.47	0.11	5	1.12 ± 0.35	$< 10.6 \times 10^{-6}$
1.6	2.37–2.42	0.10	4	0.95 ± 0.30	$< 9.6 \times 10^{-6}$
1.7	2.34–2.39	0.10	1	1.09 ± 0.34	$< 4.0 \times 10^{-6}$
1.8	2.31–2.37	0.11	1	1.49 ± 0.46	$< 3.3 \times 10^{-6}$

parameter ξ_l

$$\xi_l = \lambda'^2_{l13}\left(\frac{1}{2M^2_{\tilde{l}}} + \frac{1}{12M^2_{\tilde{u}_L}} + \frac{1}{6M^2_{\tilde{b}_R}}\right)^2 = \frac{8\pi(m_u+m_b)^2\mathcal{B}(B^+\to l^+X^0)}{\tau_{B^+}g'^2f_B^2m_{B^+}^2p_l^B(m_{B^+}^2-m_l^2-m_{X^0}^2)} \quad (2)$$

where λ' is a dimensionless R-parity-violating coupling constant, g' the weak coupling constant, f_B the decay constant of the B^+ meson, m_{B^+} its mass, p_l^B the momentum of the l^+ in the B rest frame, m_u and m_b the up and bottom quark mass, m_l the charged lepton mass, m_{X^0} the neutralino mass, and $M_{\tilde{f}}$ the sfermion mass that appears as an intermediate particle. The range of upper bounds of ξ_e is 4.1×10^{-14} to $1.7 \times 10^{-13}\,\mathrm{GeV}^{-4}c^8$ and on ξ_μ is 4.2×10^{-14} to $2.3 \times 10^{-13}\,\mathrm{GeV}^{-4}c^8$.

In summary, we obtain first upper limits for the branching fraction of $B^+ \to e^+X^0$ and $B^+ \to \mu^+X^0$ for an X^0 mass range $0.1\,\mathrm{GeV}/c^2$ to $1.8\,\mathrm{GeV}/c^2$ using Belle's full data set, where X^0 is assumed to leave no experimental signature. For 18 assumed values of M_{X^0} for both modes, upper limits of branching fraction are found to be $O(10^{-6})$.

We thank the KEKB group for the excellent operation of the accelerator; the KEK cryogenics group for the efficient operation of the solenoid; and the KEK computer group, the National Institute of Informatics,

TABLE II: Fit functions for background modes.

Background	$B^+ \to e^+ X^0$	$B^+ \to \mu^+ X^0$
$b \to c$	Gaussian	Gaussian
$b \to ul\nu_l$	Asymmetric Gaussian	Gaussian
$b \to u, d, s$, leptonic	Exponential	Exponential + ARGUS [17]
$B^+ \to l\nu_l\gamma$	Asymmetric Gaussian	Asymmetric Gaussian
$B^+ \to \pi^0 l\nu_l$	Asymmetric Gaussian + Gaussian	Asymmetric Gaussian + Gaussian
$B^+ \to \pi^+ K^0$		Gaussian + Gaussian

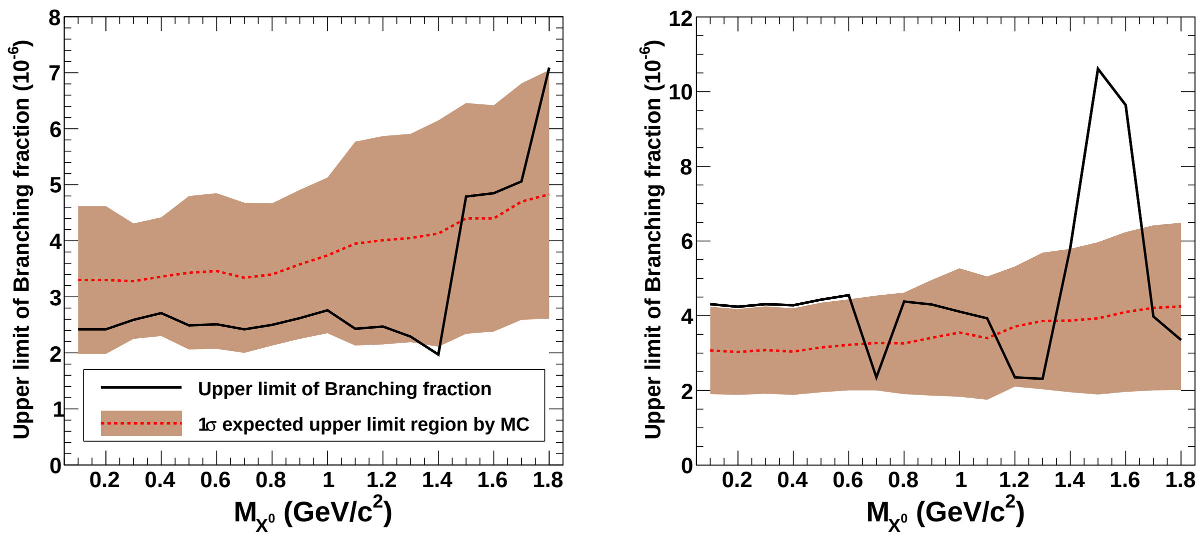

FIG. 4: The branching fraction upper limit as a function of M_{X^0} and expected upper limit with 1σ band; e mode (left) and μ mode (right).

TABLE III: Summary of multiplicative systematic uncertainties on $\epsilon_s \cdot N_{B^+B^-}$. The lepton identification and MC statistical uncertainties depend on M_{X^0} and are given as ranges.

Source	$B^+ \to e^+ X^0$	$B^+ \to \mu^+ X^0$
$N_{B^+B^-}$	1.8%	1.8%
Tracking	0.35%	0.35%
ϵ_{tag} correction	6.4%	6.4%
p_l^B shape	3.6%	3.6%
Lepton ID	(1.0–1.1)%	(0.8–0.9)%
MC sample size	(1.8–2.0)%	(1.8–1.9)%
Total	7.9%	7.8%

and the PNNL/EMSL computing group for valuable computing and SINET4 network support. We acknowledge support from the Ministry of Education, Culture, Sports, Science, and Technology (MEXT) of Japan, the Japan Society for the Promotion of Science (JSPS), and the Tau-Lepton Physics Research Center of Nagoya University; the Australian Research Council; Austrian Science Fund under Grant No. P 22742-N16 and P 26794-N20; the National Natural Science Foundation of China under Contracts No. 10575109, No. 10775142, No. 10875115, No. 11175187, No. 11475187 and No. 11575017; the Chinese Academy of Science Center for Excellence in Particle Physics; the Ministry of Education, Youth and Sports of the Czech Republic under Contract No. LG14034; the Carl Zeiss Foundation, the Deutsche Forschungsgemeinschaft, the Excellence Cluster Universe, and the VolkswagenStiftung; the Department of Science and Technology of India; the Istituto Nazionale di Fisica Nucleare of Italy; the WCU program of the Ministry of Education, National Research Foundation (NRF) of Korea Grants No. 2011-0029457, No. 2012-0008143, No. 2012R1A1A2008330, No. 2013R1A1A3007772, No. 2014R1A2A2A01005286, No. 2014R1A2A2A01002734, No. 2015R1A2A2A01003280, No. 2015H1A2A1033649, No. 2016R1D1A1B01010135; Center for Korean J-PARC Users, No. NRF-2013K1A3A7A06056592; the Brain Korea 21-Plus program and Radiation Science Research Institute; the Polish Ministry of Science and Higher Education and the National Science Center; the Ministry of Education and Science of the Russian Federation and the Russian Foundation for Basic Research; the Slovenian Research Agency; Ikerbasque,

Basque Foundation for Science and the Euskal Herriko Unibertsitatea (UPV/EHU) under program UFI 11/55 (Spain); the Swiss National Science Foundation; the Ministry of Education and the Ministry of Science and Technology of Taiwan; and the U.S. Department of Energy and the National Science Foundation. This work is supported by a Grant-in-Aid from MEXT for Science Research in a Priority Area ("New Development of Flavor Physics") and from JSPS for Creative Scientific Research ("Evolution of Tau-lepton Physics").

---

[1] W. Pauli, in *Rapp. Septieme Conseil Phys. Solvay, Brussels 1933* (Gautier-Villars, Paris, 1934).

[2] C. L. Cowan, Jr., F. Reines, F. B. Harrison, H. W. Kruse, and A. D. McGurie, Science **124**, 3212 (1956).

[3] Y. Fukuda *et al.* (Super-Kamiokande Collaboration), Phys. Rev. Lett. **81**, 1158 (1998) arXiv:hep-ex/9805021; Q. R. Ahmad *et al.* (SNO Collaboration), Phys. Rev. Lett. **87**, 071301 (2001) arXiv:nucl-ex/0106015.

[4] T. Yanagida, in Proc. of the Workshop on "The Unified Theory and Baryon Number in the Universe", Tsukuba, Japan (1979) p.95; M. Gell-Mann, P. Ramond and R. Slansky, in Supergravity, eds. P. van Nieuwenhuizen *et al.*, (North-Holland, 1979), p. 315; P. Minkowski, Phys. Lett. B **67** (1977) 421.

[5] Charge-conjugate decays are implied throughout this paper unless otherwise stated.

[6] K. Agashe, N. G. Deshpande, and G.-H. Wu, Phys. Lett. B **489**, 367 (2000) arXiv:hep-ph/0006122.

[7] D. Gorbunov and M. Shaposhnikov, J. High Energy Phys. 10 (2007) 015 arXiv:0705.1729.

[8] A. Dedes and H. Dreiner, Phys. Rev. D **65**, 015001 (2001) arXiv:hep-ph/0106199

[9] S. Kurokawa and E. Kikutani, Nucl. Instrum. Methods Phys. Res. Sect. A **499**, 1 (2003), and other papers included in this Volume; T.Abe *et al.*, Prog. Theor. Exp. Phys. (2013) 03A001 and following articles up to 03A011.

[10] A. J. Bevan *et al.*, Eur. Phys. J. C **74**, (2014) 3026 arXiv:1406.6311.

[11] M. Feindt *et al.* (Belle Collaboration), Nucl. Instrum. Methods Phys. Res., Sect. A **654**, 432 (2011) arXiv:1102.3876.

[12] A. Sibidanov *et al.* (Belle Collaboration), Phys. Rev. D **88**, 032005 (2013) arXiv:1306.2781.

[13] Y. Yook *et al.* (Belle Collaboration), Phys. Rev. D **91**, 052016 (2015) arXiv:1406.6356.

[14] K. Hanagaki *et al.*, Nucl. Instrum. Methods Phys. Res., Sect. A **485**, 490 (2002); A. Abashian *et al.*, Nucl. Instrum. Methods Phys. Res., Sect. A **491**, 69 (2002).

[15] S. Brandt *et al.*, Phys. Lett. **12** (1964) 57.

[16] A. Heller *et al.* (Belle Collaboration), Phys. Rev. D **91** (2015) 112009 arXiv:1504.05831.

[17] H. Albrecht *et al.* (ARGUS Collaboration), Phys. Lett. B **241** (1990) 278.

[18] D. J. Lange, Nucl. Instrum. Methods Phys. Res., Sect. A **462**, 152 (2001).

[19] E. Barberio and Z. Wąs, Comput. Phys. Commun. **79**, 291 (1994).

[20] R. Brun *et al.*, GEANT3.21, CERN Report DD/EE/84-1 (1984).

[21] G. J. Feldman and R. D. Cousins, Phys. Rev. D **57**, 3873 (1998).

[22] J. Conrad *et al.*, Phys. Rev. D **67**, 012002 (2003).

[23] K. A. Olive *et al.* (Particle Data Group), Chin. Phys. C, **38**, 090001 (2014)